Bioorganic & Medicinal Chemistry 17 (2009) 7197–7208

Contents lists available at ScienceDirect

Bioorganic & Medicinal Chemistry

journal homepage: www.elsevier.com/locate/bmc

PET-compatible endothelin receptor radioligands: Synthesis and first in vitro and in vivo studies

Carsten Höltke [a,b,*], Marilyn P. Law [a], Stefan Wagner [a], Klaus Kopka [a,c,d], Andreas Faust [a,b], Hans-Jörg Breyholz [a], Otmar Schober [a], Christoph Bremer [b,c], Burkhard Riemann [a], Michael Schäfers [c,d]

[a] Department of Nuclear Medicine, Albert-Schweitzer-Str. 33, University Hospital Münster, D-48149 Münster, Germany
[b] Department of Clinical Radiology, Albert-Schweitzer-Str. 33, University Hospital Münster, D-48149 Münster, Germany
[c] Interdisciplinary Center for Clinical Research (IZKF Münster), University of Münster, D-48149 Münster, Germany
[d] European Institute of Molecular Imaging (EIMI), University of Münster, D-48149 Münster, Germany

ARTICLE INFO

Article history:
Received 10 June 2009
Revised 12 August 2009
Accepted 28 August 2009
Available online 2 September 2009

Keywords:
Endothelin axis
Radiofluorination
PET imaging
Biodistribution studies
Binding studies

ABSTRACT

The expression and function of endothelin (ET) receptors is abnormal in cardiovascular diseases, tumor progression, and tumor metastasis. In this study, we prepared two [^{18}F]-fluorinated derivatives of the non-peptide ET_A receptor antagonist PD 156707 and evaluated their ET receptor binding potencies. Ex vivo as well as in vivo biodistribution studies in mice were performed, as well as the metabolism of the radiotracer, which was examined by metabolite analysis in mice and rats. All tested derivatives of PD 156707 exhibited potent in vitro pharmacological characteristics with K_i values comparable to that of the lead compound. The biodistribution studies showed a high accumulation of the tracer in bile and intestine. In vivo we were able to show that the visualization of the heart as a major target organ with high ET_AR expression is possible.

1. Introduction

Endothelin (ET) was first described by Hickey et al.[1] and subsequently isolated by Yanagisawa et al.[2] as a 21-amino acid peptide with vasoactive potential. Subsequent studies explored the role of the endothelins in a manifold of vascular diseases, including pulmonary arterial hypertension, atherosclerosis, and congestive heart failure.[3–8] In addition, the role of endothelin as an angiogenic stimulus in a number of oncologic pathologies has recently been described.[9–13]

Three isoforms of the endothelin peptides exist (ET-1, ET-2, and ET-3), exerting their effects via two associated G-protein coupled receptors (ET_AR, ET_BR). While ET_AR is primarily located on vascular smooth muscle cells and is responsible for vasoconstriction and cell proliferation, ET_BR is located on smooth muscle cells and vascular endothelial cells, causing vasodilation by the release of nitric oxide and prostacyclin and is responsible for the clearance of ET-1 from plasma in, for example, lung tissue.[14–18] This system of the three endothelin peptides and the two endothelin receptors is referred to as the endothelin axis.[11]

In some examples of mouse models of human atherosclerosis (e.g., apolipoprotein E-deficient mice)[19–22] as well as in different cases of cancer[23–27] ET receptor density is upregulated. In this context, a method for the visualization of ET receptor density in affected tissue would be highly valuable for clinical diagnosis and the evaluation of therapy. The method of choice for imaging receptor distribution in vivo is positron emission tomography (PET). The radiolabeling of ET receptor agonists and antagonists for in vivo imaging studies using PET has been reported. [^{11}C]L-753037, a 1,3-bisarylindane-2-carboxylic acid based non-selective ET receptor ligand, has been used for the in vivo imaging of ET receptors in a dog heart.[28] Another representative of this compound class (SB-209670) has been radiofluorinated for imaging ET receptor distribution in rats.[29] The widely used ET_A receptor selective ligand Atrasentan (ABT 627) was radiomethylated and has been utilized for the PET imaging of the ET_A distribution in a baboon.[30] Recently, two different ET_AR antagonists derived from BMS 207940 were radiolabeled with [^{18}F]fluoride and [^{11}C]CH_3I, respectively, and used for in vivo PET imaging in a baboon.[31] Interestingly, none of these approaches has been applied to in vivo imaging of ET receptors in humans so far. Therefore, there is still a strong motivation for research toward ET receptor radioligands for clinical applications. PD 156707 (3-benzo[1,3]dioxol-5-yl-5-hydroxy-5-(4-methoxyphenyl)-4-(3,4,5-trimethoxybenzyl)-5*H*-furan-2-one) and related butenolide derivatives are potent ET receptor antagonists with both

* Corresponding author at present address: Department of Nuclear Medicine, Radiochemistry, Albert-Schweitzer-Str. 33, University Hospital Münster, 48149 Münster, Germany. Tel.: +49 251 8347362; fax: +49 251 8347363.
E-mail address: carsten.hoeltke@uni-muenster.de (C. Höltke).

0968-0896/$ - see front matter © 2009 Elsevier Ltd. All rights reserved.
doi:10.1016/j.bmc.2009.08.058

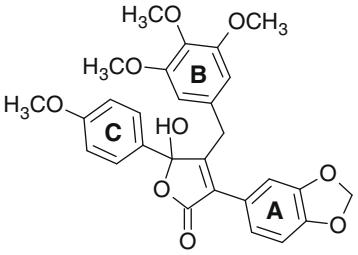

Figure 1. Structure of lead compound PD 156707.

high affinity and ET_AR selectivity.[32,33] In this study we describe the synthesis and first in vivo evaluation of radiofluorinated derivatives of this compound.

2. Results and discussion

The objective of this work was the modification of an existing lead structure (PD 156707, Fig. 1) with the PET-compatible radionuclide [^{18}F]fluorine for the detection and quantification of ET_A receptors in PET examinations. We have chosen a one-step radiolabeling procedure using [^{18}F]K(Kryptofix 2.2.2)F and tosylate precursor compounds. Suitable positions for the placement of these leaving groups are found on aromatic rings B and C of the lead compound (Fig. 1), where a methoxy group can be replaced by an adequately substituted ethoxy group. This approach leads to two distinct radiofluorination precursors. The two non-radioactive ^{19}F-substituted reference compounds were synthesized by similar strategies.

2.1. Chemistry

Key intermediates of all four target compounds are the γ-keto esters **1**(**a**–**c**), **2** and **3** and the benzaldehydes **4**–**6** (Schemes 1 and 2). The γ-ketoesters **1**–**3** were prepared following procedures described by Patt et al.,[33] where the preparation of **1a** is illustrated. Replacing the methoxy group with a benzyl group yields γ-ketoester **1b**, which enables subsequent hydrogenolysis to γ-ketoester **1c**.[34] Re-substitution reactions with dibromoethane or (2-fluoroethyl)-4-methylbenzene sulfonate yield the desired γ-ketoesters **2** and **3** (Scheme 1) in ≈60% yield. 3,4,5-Trimethoxybenzaldehyde **4** is commercially available, aldehydes **5** and **6** were synthesized starting from 3,4-dimethoxy-5-hydroxybenzaldehyde and dibromoethane or (2-fluoroethyl)-4-methylbenzene sulfonate, respectively (Scheme 2). Reactions were conducted in dimethylformamide as solvent and with cesium carbonate as base. Product yields were 65–73% in case of **5** and 69–93% for **6**. The higher yields of **6** were always obtained when dibromoethane was used in excess. The coupling of the benzaldehydes and the γ-ketoesters is realized by an aldol condensation, saponification and cyclization sequence. This conversion requires refluxing with sodium methoxide in methanol for several hours followed by acidification of the reaction mixture with acetic acid and further refluxing. The butenolides **7**–**10** (Scheme 3) were obtained in 29–53% yield. Multiple byproducts were detected by TLC. Derivatives **7** and **9** are the desired non-radioactive reference compounds with ^{19}F-fluoroethoxy substitution. For the preparation of the radiolabeling precursors, the two bromoethoxy-substituted butenolides **8** and **10** are heated to reflux with an excess of silver tosylate in acetonitrile, yielding the tosylates **11** and **12** in ≈80% yield. Conversions at 150 °C with less silver tosylate and DMF as solvent were always less efficient (data not shown).

2.2. Radiochemistry

The two precursor tosylates **11** and **12** were converted into the [^{18}F]-substituted target compounds **[^{18}F]7** and **[^{18}F]9** using [^{18}F]K(Kryptofix 2.2.2)F and potassium carbonate in acetonitrile (Scheme 4). Compound **[^{18}F]7** was produced with a radiochemical yield of 21.4 ± 6.1% (noted as mean ± SD, decay-corrected, n = 12). The synthesis was achieved with a radiochemical purity of 98.1 ± 0.8% in 71 ± 2 min from end of radionuclide production and a calculated specific radioactivity of 35–50 GBq/μmol at the end of synthesis (EOS, n = 12). Besides the injection peak the UV-trace of the HPLC quality control of the purified **[^{18}F]7** fraction showed only an additional peak for the carrier, from which the specific radioactivity was calculated. Compound **[^{18}F]9** was produced by the same procedure as **[^{18}F]7**. Due to the higher in vitro potency of **7** compared to **9** (see below) an optimization of the radiosynthesis of **[^{18}F]9** was not performed. Thus, the number of experiments

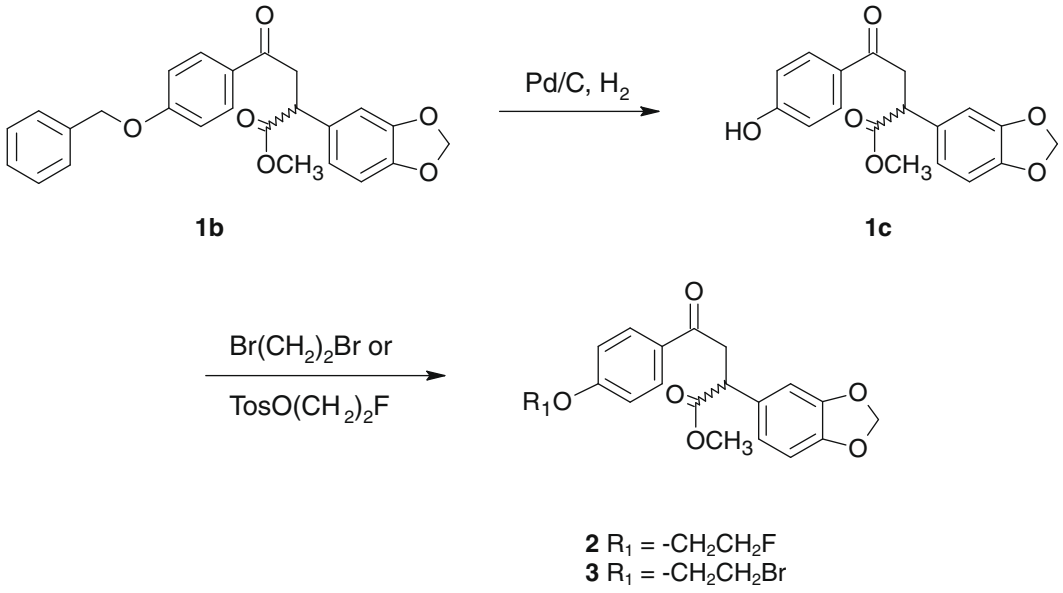

Scheme 1. Preparation of γ-ketoesters **2** and **3** starting from benzyl protected **1b**. Hydrogenation yields the phenoxy derivative **1c**, which subsequently is converted to the haloethoxy products **2** and **3**.

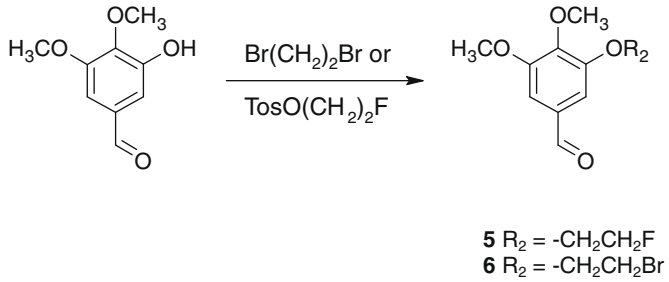

Scheme 2. Synthesis of haloethoxy benzaldehydes **5** and **6** from commercially available 3,4-dimethoxy-5-hydroxy benzaldehyde.

was reduced ($n = 3$), just to prove the possibility for a radioconversion of the tosylate precursor **12** to the radiolabeled product **[^{18}F]9**.

2.3. Biology

In vitro determination of receptor affinity and selectivity: The affinities of the prepared butenolide derivatives **7**–**12** toward endothelin receptors were determined by competition binding studies using [^{125}I]ET-1 and mouse ventricular membrane preparations. The binding of the non-selective ET receptor ligand [^{125}I]ET-1 to ventricular membranes was specific, saturable and of high affinity. Values for the dissociation constant ($K_D = 208 \pm 2$ pM) and the maximum number of binding sites ($B_{max} = 300 \pm 3$ fmol/mg

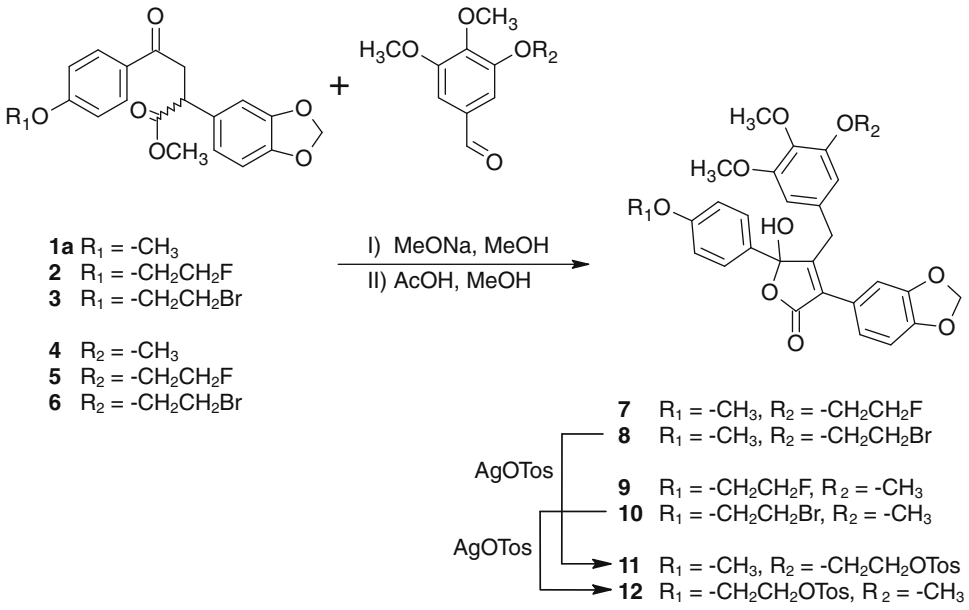

Scheme 3. Aldol condensation of γ-ketoesters **1**–**3** with benzaldehydes **4**–**6** and subsequent cyclization, yielding the butenolides **7**–**10**. The bromo derivatives **8** and **10** are further converted to the radiofluorination precursor tosylates **11** and **12** by reaction with silver tosylate.

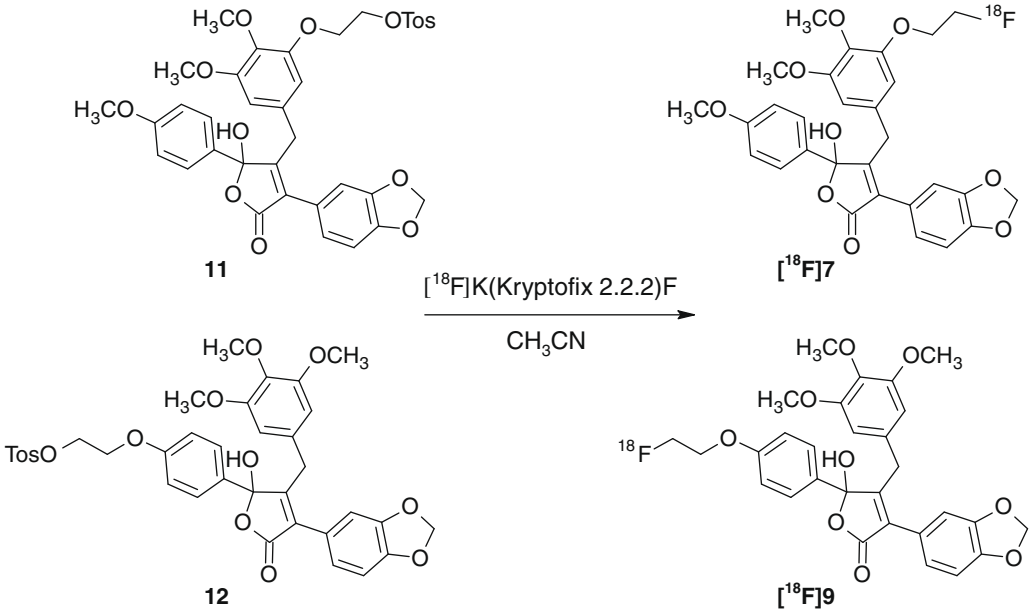

Scheme 4. Radiofluorination reactions of the precursor tosylates with [^{18}F]K(Kryptofix 2.2.2)F.

Table 1
Affinities of the prepared compounds toward endothelin receptors given as mean ± SEM (n = 3)

Structure	Weight	Affinities (nM) ± SEM[a]	Selectivity	Log D_{calc}
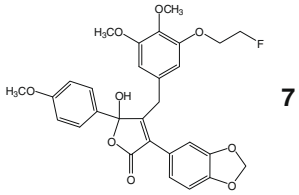 **7**	538.52	$K_i(ET_A)$ = 1.09 ± 0.60 $K_i(ET_B)$ = 240 ± 16	218:1	3.51
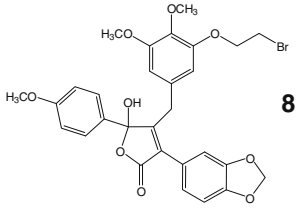 **8**	599.42	$K_i(ET_A)$ = 0.24 ± 0.10 $K_i(ET_B)$ = 170 ± 50	708:1	4.05
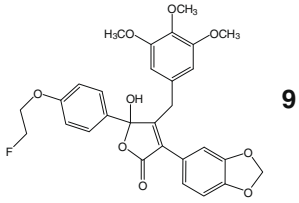 **9**	538.52	$K_i(ET_A)$ = 2.43 ± 0.95 $K_i(ET_B)$ = 98 ± 53	40:1	3.51
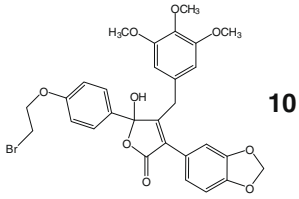 **10**	599.42	$K_i(ET_A)$ = 25 ± 2.7 $K_i(ET_B)$ = 72 ± 52	3:1	4.05
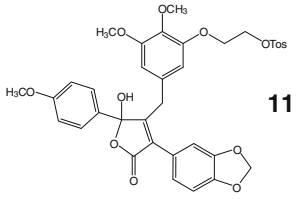 **11**	690.71	$K_i(ET_A)$ = 1.26 ± 0.81 $K_i(ET_B)$ = 1.26 ± 0.81	1:1	4.37
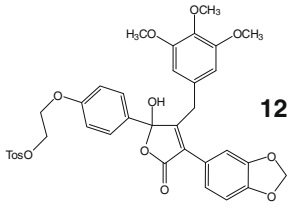 **12**	690.71	$K_i(ET_A)$ = 0.36 ± 0.15 $K_i(ET_B)$ = 96 ± 51	267:1	4.37
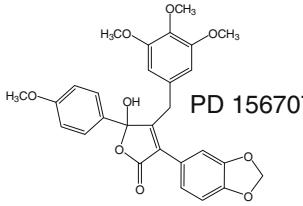 PD 156707	506.50	$IC_{50}(ET_A)$ = 0.3[b] $IC_{50}(ET_B)$ = 780[b]	2600:1	3.29

The IC_{50} values of the lead compound PD 156707 are given for comparison. Selectivities are given as $K_i(ET_B)/K_i(ET_A)$ and $IC_{50}(ET_B)/IC_{50}(ET_A)$ in case of PD 156707. Log D values were calculated using the Log D Suite program by ACDLabs/ChemSketch 6.0 distribution (log D = log P at pH 7.4).

[a] n = 3

[b] IC_{50} values from Patt et al. *J. Med. Chem.* **1997**, *40*, 1063.

protein) were used for the calculations as previously determined.[34] Different concentrations of the prepared compounds were incubated with [^{125}I]ET-1 and a fixed amount of mouse ventricular membranes. The membrane bound radioactivity was evaluated using a γ-scintillation counter. Non-linear regression analysis showed that the data of the compounds fitted a two-site model. This model assumes that the ligand binds to two receptor subtypes with two different affinities, resulting in a high- and a low-affinity inhibition constants K_i(high) and K_i(low). In the case of endothelin receptors most ligands are known to be ET_AR selective, so the high-affinity constant describes the interaction of the ligand with the ET_AR subtype and the low-affinity constant that with the ET_BR subtype. The high- and low-affinity inhibition constants $K_i(ET_A)$ and $K_i(ET_B)$ are displayed in Table 1. For comparison, the values of the lead compound PD 156707 are also given as published.[33] All prepared butenolide derivatives show a high affinity to ET receptors with K_i values ranging from 0.24 to 240 nM. Except for precursor tosylate **11** all compounds exhibit higher affinities to ET_AR than to ET_BR with ratios for $K_i(ET_B)/K_i(ET_A)$ from ≈3.0 for compound **10** to ≈700 for compound **8**. Interestingly, the site of modification (para-substituted phenyl vs 5-substituted dimethoxy-benzyl) is not largely influencing the affinities. The target compounds with fluoroethoxy substitution **7** and **9** show affinities to the ET_A receptor of 1.1 and 2.4 nM, respectively, proving the possibility to exchange an aromatic methoxy function with a 2-fluoroethoxy group without profoundly decreasing the receptor affinity. However, the selectivities of the ligands suffer from this modification. For this reason, we chose **[^{18}F]7** for in vivo and ex vivo experiments. This ligand still displays a selectivity to the ET_A receptor of 220:1, compared to a ratio of only 40:1 for **9**. Notably, compound **9**, with the fluoroethoxy substitution on the phenyl-site, shows an ET_AR affinity 10 times that of the comparable bromoethoxy-substituted compound **10**, while the affinity values are reversed when looking at the benzyl-substituted compounds **7** and **8**. Bromoethoxy compound **8** is about five times more affine to ET_AR than fluoroethoxy derivative **7** and also shows the highest selectivity with $K_i(ET_B)/K_i(ET_A) \approx 700$.

Ex vivo biodistribution studies in mice: All animal studies were performed with **[^{18}F]7**. Upon intravenous administration of the radiotracer, high levels of radioactivity were found in liver, lung, bile, and duodenum (Fig. 2). Uptake into the brain was negligible, indicating that the radiotracer is not passing the blood–brain-barrier, and uptake indices for spleen and muscle were lower than that for plasma. Uptake indices for other tissues were higher than that for plasma at early times. Relatively low levels of radioactivity were detected in urine but an exceptionally high concentration of radioactivity was seen in bile. Time activity curves (Fig. 2) show that in all tissues except duodenum highest levels of radioactivity were detected at the first sampling time (2 min). Subsequently, radioactivity cleared rapidly from tissues. The values for duodenum indicate an increase in radioactivity between 2 and 5 min after injection of **[^{18}F]7** followed by a slow loss, which may be related to the excretion of radioactivity into the bile. The radioactivity in the duodenal contents was assessed at 30 min by transferring the contents directly into weighed vials. Radioactivity of the contents was high (uptake index 33 ± 7, $n = 5$) compared to that of the duodenal wall (uptake index 9 ± 2, $n = 7$).

Predosing mice with the ET_AR selective antagonist PD 156707 slightly reduced the uptake indices for all tissues except for plasma and duodenum which showed no changes and stomach which showed a small increase (Fig. 3). The differences were significant for myocardium and muscle (t-test, $p < 0.05$, $n = 7$ for each group), but the overall retention of radioactivity in the majority of tissues assessed was very low and, therefore, the differences between 'total' (no predose) and 'non-specific' (with PD 156707 predose) binding was small. An ET_A receptor targeted conjugate with the fluorescent dye Cyanine 5.5 based on the same lead structure PD 156707 has been shown to highly specifically bind to target receptors in mice.[35] Due to its high hydrophilicity, caused by the sulfonate-substituted nature of the dye, it also showed a much more favorable renal excretion profile. This leads to the assumption that a modification of the radiotracer concerning higher hydrophilicity is a possible route to a more applicable PET-tracer for the in vivo imaging of endothelin receptors.

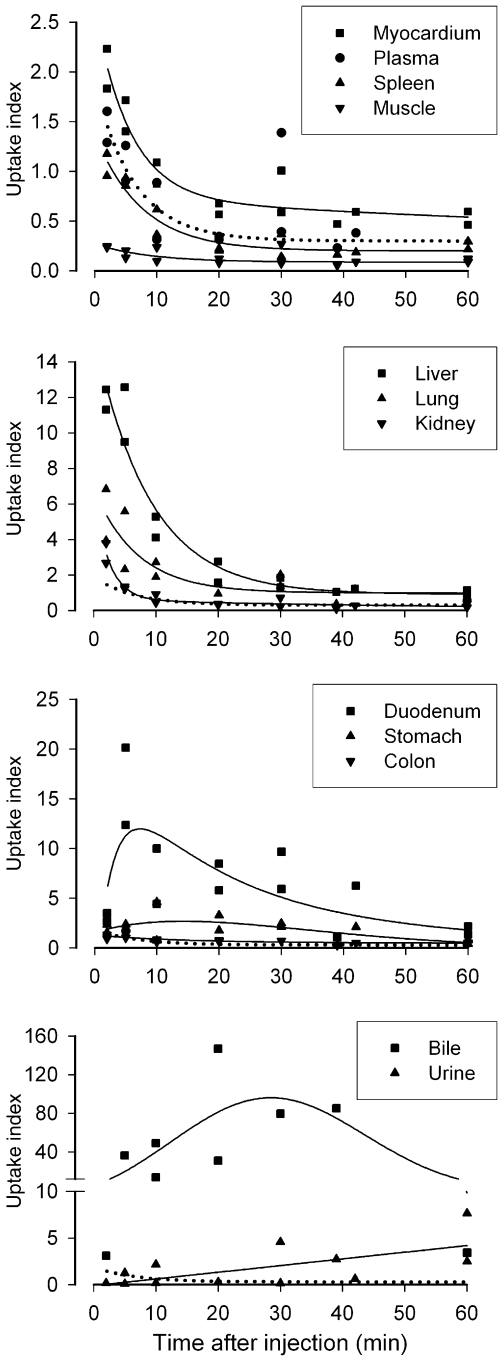

Figure 2. Radioactivity in tissues of mice after intravenous injection of **[^{18}F]7**. Each symbol represents data for an individual mouse. The lines are biexponential fits to data with the exception of duodenum, stomach, and bile which were fitted by a peak equation (Weibull, 4 Parameter, SigmaPlot) for illustration. The top panel shows results for myocardium (■), plasma (●), spleen (▲), and muscle (▼). The dotted line shows the biexponential fit to plasma data and is included in all panels. The second panel shows liver (■), lung (▲), and kidney (▼). The third panel shows duodenum (■), stomach (▲), and colon (▼). The bottom panel shows data for bile (■) and urine (▲).

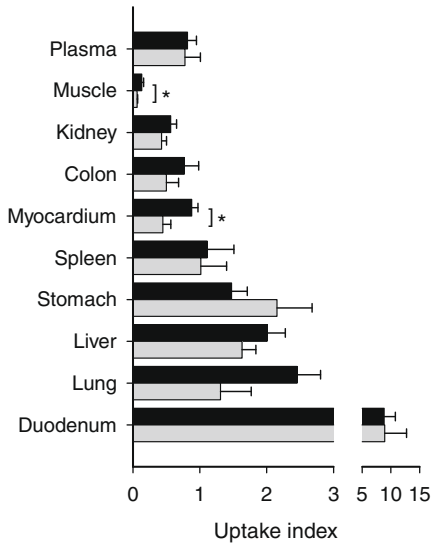

Figure 3. Effect of the ET_A receptor antagonist PD 156707 on radioactivity in tissues of mice after intravenous injection of **[^{18}F]7**. Water for injection (seven mice) or PD 156707 at 1.0 μmol/kg (seven mice) was injected 10 min before **[^{18}F]7** (<1.0 nmol/kg). Tissue radioactivity (mean uptake index with standard errors) at 30 min after **[^{18}F]7** is shown. *Significant difference (*t*-test, p <0.05). ■ Water for injection; ▭ PD 156707.

Metabolism: Preliminary studies were carried out in which rat plasma was incubated with ≈19 MBq of **[^{18}F]7** at 37 °C for 1, 2.5, 20, and 60 min. Plasma protein binding of the tracer amounted to only 4.6–6.7% of applied radioactivity. HPLC analysis of the supernatant detected only parent **[^{18}F]7**, confirming the plasma stability of the compound. Figure 4A shows results obtained for a single rat after administration of 40 MBq of **[^{18}F]7** where serial blood samples (2.5–60 min) were taken. Only parent **[^{18}F]7** was detected at 2.5 min after injection. Very low amounts of radioactivity were extracted at 10 min after injection but again only parent **[^{18}F]7** was clearly observed, although there was possibly a polar metabolite with t_R = 3.6 min. At 20 min parent **[^{18}F]7** was detected but there were at least two polar radioactive metabolites (3.6 and 4.4 min). Plasma radioactivity at 60 min was below detection limits on the used HPLC system. Radioactive metabolites (3.6, 4.5, and 6.2 min), however, were observed in urine at 60 min.

Figure 4B shows HPLC analysis of plasma and urine samples taken at 5 and 20 min after intravenous injection of **[^{18}F]7** into mice. For each time point blood from two mice was combined to give 1 ml aliquots for preparation of plasma. The urine sample was taken from one mouse and injected directly onto the HPLC system. Five minutes after injection parent **[^{18}F]7** was detected (elution time 26.0 min) in plasma but not in urine. Two more polar radioactive metabolites were detectable at 17.1 min in plasma and at 3.0 min in urine. At 20 min parent **[^{18}F]7** was still present in plasma but could not be detected in urine. One major polar radiometabolite was detectable in plasma at 3.6 min, accompanied by two faintly detectable signals at 11.7 and 17.1 min. In urine three polar metabolites could be detected at 3.2, 4.1, and 5.9 min.

These results indicate that in mice and rats the radiotracer **[^{18}F]7** is rapidly converted to polar radiometabolites which are detectable in plasma at early times after iv injection and at later times (>5 min) accumulate in urine. A possible metabolic pathway is described by Zoghbi et al. They proposed the defluoroethylation of a radiofluorinated dopamine transporter ligand, resulting in the formation of 2-[^{18}F]fluoroethanol and, in turn, its oxidation products [^{18}F]fluoroacetaldehyde and [^{18}F]fluoroacetate.[36] Furthermore, Sykes et al. described that [^{18}F]fluoroacetate is metabolized to [^{18}F]fluoride ion in mouse and rat.[37] The formation of [^{18}F]fluoride, however, is usually accompanied by an accumulation of radioactivity in the skeleton, which could not be confirmed by small-animal PET examinations (see below). The observed polar radiometabolites of **[^{18}F]7** are therefore likely to be [^{18}F]fluoroethanol and its oxidation products.

2.4. PET scans

Although myocardial uptake of radioactivity after injection of **[^{18}F]7** was low, the heart was successfully visualized by PET in vivo (Fig. 5). In conformity with the ex vivo experiments time activity curves for tissues, with the exception of the liver, showed uptake of radioactivity followed by a rapid decrease during the first 2 min, mirroring organ perfusion by radioactivity in the blood. The increase in blood activity between 10 and 20 min (Fig. 5) may reflect the re-entry of radioactivity from tissue to vascular compartments or the spillover from liver or bile due to movement of the animal. Myocardial radioactivity was found to be higher than that in blood between 2 and 15 min (heart-to-blood ratio = 1.5–3.0), but in brain, lung, spleen, muscle, and kidney it was similar to or lower than that in blood. Liver radioactivity increased to a maximum at 3–4 min and then showed a gradual decrease over the next hour. Similarly, radioactivity in the bile reached a maximum (∼6000 cps ml^{-1}) at 3–4 min and then decreased, whereas urine levels (200 cps ml^{-1}) showed very little change over 5–60 min (data not shown).

3. Conclusion

We successfully established the synthesis of two novel ET_A receptor affine radioligands by semiautomatic one-step radiofluorination procedures. The ligand (**[^{18}F]7**) was tested in biodistribution studies in rats and mice ex vivo and in vivo. Although myocardial uptake of **[^{18}F]7** as an indicator of ET_A receptor binding was low, a significant reduction in tracer uptake of target tissue could be demonstrated by predosing experiments with the ET_A receptor ligand PD 156707. Also, we were able to visualize myocardial tracer uptake by small-animal PET experiments in mice. However, the very low uptake of **[^{18}F]7** into target tissue makes it difficult to determine specificity of the tracer in vivo. The rapid metabolism into polar radiometabolites and a major hepatobiliary route of excretion are the major drawbacks for that matter. Therefore, the improvement of stability and enhancement of hydrophilicity are among the major strategies in future synthetic work. Disease models with locally upregulated expression of endothelin receptors, on the other hand, may provide a useful platform to more closely examine the binding potency of the designed tracer in vivo.

4. Experimental

4.1. General

All chemicals, reagents and solvents for the synthesis of the compounds were analytical grade and purchased from commercial sources. PD 156707 and 2-(benzo-[1,3]-dioxol-5-yl)-1-(4-benzyloxyphenyl)-4-oxobutyric acid methyl ester (**1b**) were synthesized as reported.[34,33] (2-Fluoroethyl)-4-methylbenzene sulfonate was synthesized as described by Parenty et al.[38] Melting points (uncorrected) were determined on a Stuart Scientific SMP3 capillary melting point apparatus. ^{1}H and ^{13}C NMR spectra were recorded on a Bruker ARX 300, and AMX 400 spectrometer, respectively. Mass spectrometry was performed using a Varian MAT 212 (EI = 70 eV) spectrometer and a Bruker MALDI-TOF-MS Reflex IV

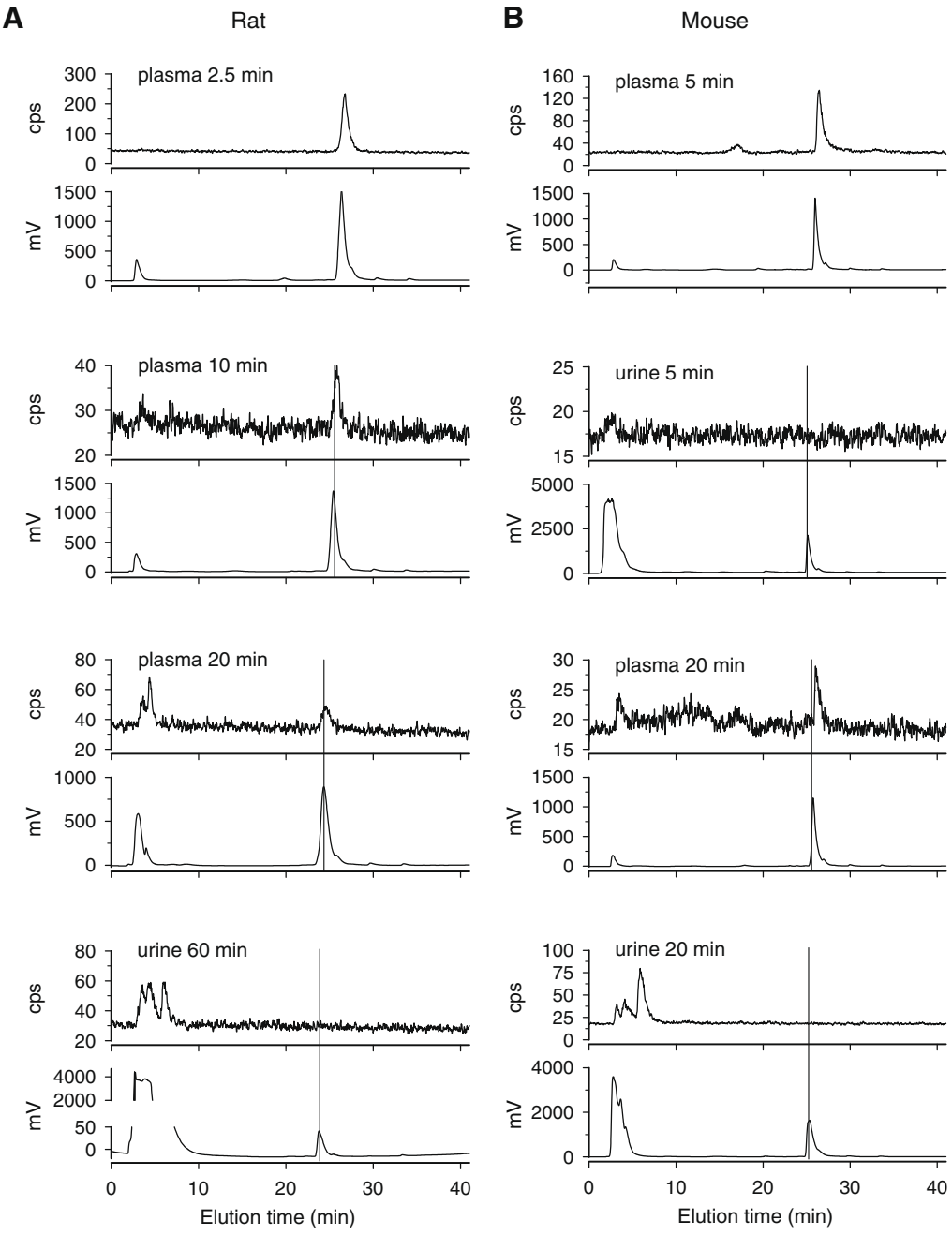

Figure 4. Rat (left) and murine (right) radio- and UV–HPLC-traces of plasma and urine samples taken at the denoted time points after tail vein injection of **[^{18}F]7**. The vertical line at ≈26 min indicates the elution time of the reference compound **7**, which has been co-injected for identification.

(matrix: DHB). Elemental analysis was realized by a Vario EL III analyzer. Separation of the radiosynthesized compounds, analyses of radiochemical yields and radiochemical purities were performed by gradient radio-RP-HPLC using a Knauer system with two K-1800 pumps, an S-2500 UV detector (Herbert Knauer GmbH, Berlin, Germany) and a RP-HPLC Nucleosil 100-5 C18 column (250 mm × 4.6 mm) coupled to a raytest GabiStar γ-detector (raytest Isotopenmessgeraete GmbH, Straubenhardt, Germany). The conditions used are described in detail below. The recorded data were processed by the ChromGate HPLC software (Knauer). Radioactivity of tissue was determined using an automated γ-counter (Wallac Wizard 3″, Perkin–Elmer Life Sciences, Boston, USA). All animal experiments were conducted in accordance with local institutional guidelines for the care and use of laboratory animals.

4.2. Chemistry

4.2.1. 2-(1,3-Benzodioxol-5-yl)-1-(4-hydroxyphenyl)-4-oxobutyric acid methyl ester 1c

An amount of 12.5 g (30.0 mmol) 2-(1,3-benzodioxol-5-yl)-1-(4-benzyloxyphenyl)-4-oxobutyric acid methyl ester (**1b**) is suspended in 200 ml of a 1:1 mixture of ethanol and ethyl acetate. To this is added 150 mg of hydrogenation catalyst (Pd/C 10%, *FLUKA*) and the mixture is stirred under a hydrogen atmosphere for 48 h. The catalyst is filtered off and the solvent is evaporated in vacuo. The remaining solid is recrystallized from methanol, giving 8.13 g of colorless crystals (24.8 mmol, 83%), mp 155 °C. ^{1}H NMR ($CDCl_3$) δ = 9.78 (br, 1H), 7.83 (d, 2H, J = 8.3 Hz), 6.85 (m, 3H), 6.75 (m, 2H), 5.90 (s, 2H), 4.35 (dd, 1H, J = 3.8 Hz, J = 10.1 Hz),

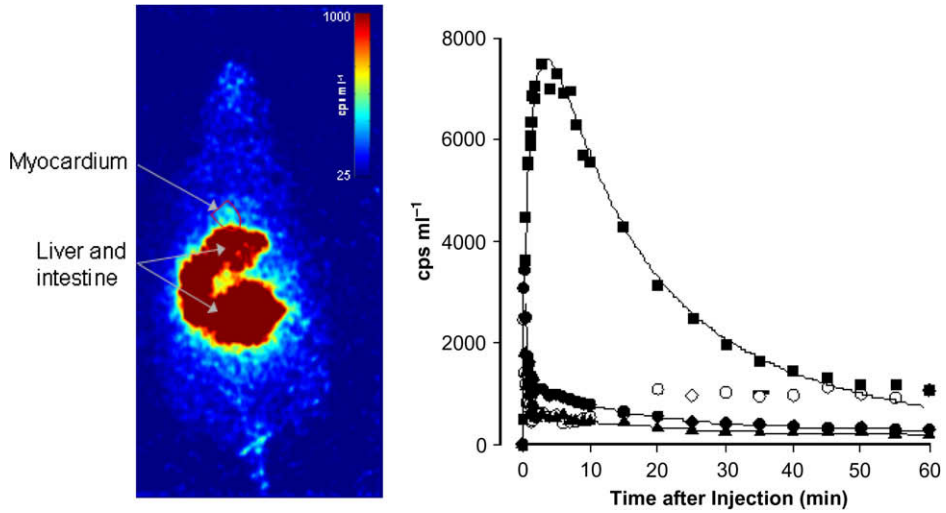

Figure 5. Small-animal PET scan of a wild type mouse (2 h pi) after tail vein injection of 6.67 MBq of **[^{18}F]7**. High signal intensity is found mainly in liver and intestine. Although uptake of radioactivity in the myocardium was low the heart could be visualized (values: cps ml^{-1}). Regions of interest were drawn in the left ventricle (blood ○), round the heart (●), in the lung (▲), and in the liver (■). Symbols indicate values (cps ml^{-1}) for each time frame, lines indicate empirical fits to the data.

3.77 (dd, 1H, J = 10.1 Hz, J = 17.8 Hz), 3.64 (s, 3H), 3.18 (dd, 1H, J = 3.8 Hz, J = 17.9 Hz) ppm. ^{13}C NMR δ = 195.0, 173.1, 161.7, 147.0, 146.0, 131.2, 129.6, 127.3, 120.2, 114.6, 107.5, 107.2, 100.2, 51.1, 45.1, 41.3 ppm. MS: m/z = 296 [M−MeOH]$^+$, 328 [M]$^+$. Anal. Calcd for $C_{18}H_{16}O_6$: C, 65.85; H, 4.91. Found: C, 65.98; H, 5.04.

4.2.2. 2-(1,3-Benzodioxol-5-yl)-1-[4-(2-fluoroethoxy)phenyl]-4-oxobutyric acid methyl ester 2

A suspension of 1.64 g (5.0 mmol) 2-(1,3-benzodioxol-5-yl)-1-(4-hydroxyphenyl)-4-oxobutyric acid methyl ester (**1c**), 1.20 g (5.5 mmol) (2-fluoroethyl)-4-methylbenzene sulfonate and 3.25 g (10.0 mmol) cesium carbonate in 50 ml of DMF are warmed to 80 °C for 1 h. The mixture is poured into 100 ml of water, neutralized with acetic acid and extracted with dichloromethane. The combined organic layers are washed with water and brine and dried over magnesium sulfate. After filtration the solvent is removed and the crude residue purified by silica gel column chromatography (cyclohexane/ethyl acetate 3/2, R_f = 0.54). Yield 1.20 g (2.93 mmol, 59%), mp 124 °C. ^{1}H NMR ($CDCl_3$) δ = 7.93 (d, 2H, J = 8.8 Hz), 6.93 (d, 2H, J = 8.8 Hz), 6.84–6.72 (m, 3H), 5.92 (s, 2H), 4.75 (dm, 2H, J = 47 Hz), 4.24 (dm, 2H, J = 28 Hz), 4.17 (dd, 1H, J = 3.6 Hz, J = 10.1 Hz), 3.81 (dd, 1H, J = 10.1 Hz, J = 18.1 Hz), 3.67 (s, 3H), 3.18 (dd, 1H, J = 3.6 Hz, J = 18.1 Hz). ^{13}C NMR ($CDCl_3$) δ = 196.0, 174.0, 162.4, 147.9, 146.9, 132.0, 130.4, 129.9, 121.1, 114.2, 108.5, 108.1, 101.1, 81.5 (d, J = 171 Hz), 67.1 (d, J = 20 Hz), 52.3, 46.0, 42.5. ^{19}F NMR ($CDCl_3$) δ = −224, MS (EI): m/z = 397 [M+Na]$^+$. Anal. Calcd for $C_{20}H_{19}FO_6$: C, 64.17; H, 5.12. Found: C, 63.98; H, 5.21.

4.2.3. 2-(1,3-Benzodioxol-5-yl)-1-[4-(2-bromoethoxy)phenyl]-4-oxobutyric acid methyl ester 3

A solution of 7.79 g (23.7 mmol) 2-(1,3-benzodioxol-5-yl)-1-(4-hydroxyphenyl)-4-oxobutyric acid methyl ester (**1c**), 30.5 g (96.6 mmol) cesium carbonate and 45.1 g (240 mmol, 20.1 ml) 1,2-dibromoethane in 150 ml of DMF are stirred at rt for 20 h. The mixture is poured into 250 ml of water which is then extracted thrice with dichloromethane. The combined organic layers are washed with brine, dried over magnesium sulfate and filtered. After removal of the solvent the residue is chromatographed on silica gel (cyclohexane/ethyl acetate 7/3, R_f = 0.48) yielding 6.60 g (15.2 mmol, 64%) of the product as colorless crystals, mp 112 °C. ^{1}H NMR ($CDCl_3$) δ = 7.94 (d, 2H, J = 9.0 Hz), 6.93 (d, 2H, J = 9.0 Hz), 6.85–6.74 (m, 3H), 5.93 (s, 2H), 4.34 (t, 2H, J = 6.1 Hz), 4.19 (dd, 1H, J = 4.1 Hz, J = 10.2 Hz), 3.82 (dd, 1H, J = 10.2 Hz, J = 17.9 Hz), 3.68 (s, 3H), 3.65 (t, 2H, J = 6.1 Hz), 3.20 (dd, 1H, J = 4.1 Hz, J = 17.9 Hz). ^{13}C NMR ($CDCl_3$) δ = 196.0, 173.9, 162.1, 148.0, 147.0, 132.1, 130.4, 130.2, 121.1, 114.4, 108.5, 108.2, 101.2, 67.9, 52.3, 46.0, 42.5, 28.6. MS (EI): m/z = 459 [M+Na]$^+$ (^{81}Br), 457 [M+Na]$^+$ (^{79}Br), 437 [M+H]$^+$ (^{81}Br), 435 [M+H]$^+$ (^{79}Br), 282, 234. Anal. Calcd for $C_{20}H_{19}BrO_6$: C, 55.19; H, 4.40. Found: C, 55.20; H, 4.43.

4.2.4. 3-(2-Fluoroethoxy)-4,5-dimethoxybenzaldehyde 5

A mixture of 1.00 g (5.00 mmol) 3,4-dimethoxy-5-hydroxybenzaldehyde, 1.79 g (5.5 mmol) cesium carbonate and 1.20 g (5.5 mmol) (2-fluoroethyl)-4-methylbenzene sulfonate in 50 ml of DMF is heated to 80 °C for 4 h. The mixture is poured into 150 ml of diluted, ice-cold hydrogen chloride solution which is then extracted thrice with ethyl acetate. The combined organic layers are washed with brine, dried over magnesium sulfate and filtered. After removal of the solvent the residue is chromatographed on silica gel (petroleum ether/ethyl acetate 2/1, R_f = 0.41) yielding 810 mg (3.55 mmol, 65%) of the product as a clear oil, which solidifies after 1 day at rt, mp 44 °C. ^{1}H NMR ($CDCl_3$) δ = 9.85 (s, 1H), 7.16 (d, 1H, J = 1.6 Hz), 7.13 (d, 1H, J = 1.6 Hz), 4.77 (dm, 2H, J = 47 Hz), 4.33 (dm, 2H, J = 28 Hz), 3.96 (s, 3H), 3.93 (s, 3H). ^{13}C NMR ($CDCl_3$) δ = 190.6, 154.0, 152.5, 142.0, 131.7, 109.1, 107.3, 81.8 (d, J = 171 Hz), 68.7 (d, J = 21 Hz), 61.1, 56.4. ^{19}F NMR ($CDCl_3$) δ = −224.0. MS (EI): m/z = 228 M$^+$. Anal. Calcd for $C_{11}H_{13}FO_4$: C, 57.89; H, 5.74. Found: C, 57.74; H, 5.56.

4.2.5. 3-(2-Bromoethoxy)-4,5-dimethoxybenzaldehyde 6

A mixture of 1.04 g (5.70 mmol) 3,4-dimethoxy-5-hydroxybenzaldehyde, 9.30 g (28.5 mmol) cesium carbonate and 10.7 g (4.9 ml, 57.0 mmol) 1,2-dibromoethane in 50 ml of DMF is stirred at rt for 3 h. The mixture is poured into 150 ml of aqueous saturated ammonium chloride solution which is then extracted thrice with dichloromethane. The combined organic layers are washed with brine, dried over magnesium sulfate and filtered. After removal of the solvent the residue is chromatographed on silica gel (cyclohexane/ethyl acetate 2/1, R_f = 0.34) yielding 1.14 g (3.94 mmol, 69%) of the product as a clear yellowish oil. ^{1}H NMR ($CDCl_3$) δ = 9.84 (s, 1H), 7.13 (d, 1H, J = 1.6 Hz), 7.08 (d, 1H, J = 1.6 Hz), 4.37 (t, 2H, J = 6.1 Hz), 3.95 (s, 3H), 3.90 (s, 3H), 3.67 (t, 2H, J = 6.1 Hz). ^{13}C NMR ($CDCl_3$) δ = 190.6, 153.9, 152.0, 144.3,

131.6, 108.9, 107.2, 69.2, 61.1, 56.2, 28.9. MS (EI): m/z = 290 M^+ (^{81}Br), 288 M^+ (^{79}Br), 181 $[M-CH_2CH_2Br]^+$, 109 $[CH_2CH_2{}^{81}Br]^+$, 107 $[CH_2CH_2{}^{79}Br]^+$. Anal. Calcd for $C_{11}H_{13}BrO_4$: C, 45.70; H, 4.53. Found: C, 45.57; H, 4.70.

4.2.6. 3-Benzo[1,3]dioxol-5-yl-4-[3-(2-fluoroethoxy)-4,5-dimethoxybenzyl]-5-hydroxy-5-(4-methoxyphenyl)-5H-furan-2-one 7

To a suspension of 1.21 g (3.54 mmol) of 2-(1,3-benzodioxol-5-yl)-1-(4-methoxyphenyl)-4-oxobutyric acid methyl ester **1a** and 195 mg (3.60 mmol) sodium methylate in 40 ml methanol 810 mg (3.55 mmol) of 3-(2-fluoroethoxy)-4,5-dimethoxybenzaldehyde **5** are added. The mixture is refluxed for 12 h under argon. Acetic acid (≈1.6 ml) is added and the mixture is further refluxed for additional 5 h. The reaction mixture is poured onto ice and extracted with ethyl acetate. The combined organic phases are washed with saturated bicarbonate solution and brine and dried over magnesium sulfate. After filtration and removal of the solvent the residue is chromatographed on silica gel (petroleum ether/ethyl acetate 1/1) to yield 820 mg (1.52 mmol, 43%) of the product as a light yellow powder, mp 66 °C (decomp.). ^1H NMR ($CDCl_3$) δ = 7.37 (d, 2H, J = 8.9 Hz), 6.91 (dd, 1H, J = 8.1 Hz, J = 1.7 Hz), 6.88 (d, 1H, J = 1.7 Hz), 6.82 (d, 2H, J = 8.9 Hz), 6.78 (d, 1H, J = 8.1 Hz), 6.02 (d, 1H, J = 1.8 Hz), 6.00 (d, 1H, J = 1.8 Hz), 5.95 (s, 2H), 4.66 (dm, 2H, J = 47 Hz), 4.60 (s, br, 1H), 3.99 (dm, 2H, J = 28 Hz), 3.78 (s, 3H), 3.74 (s, 3H), 3.65 (d, 2H, J = 2.8 Hz), 3.62 (s, 3H). ^{13}C NMR ($CDCl_3$) δ = 171.1, 160.5, 160.4, 153.2, 151.8, 148.2, 147.8, 137.5, 131.9, 128.8, 128.3, 127.5, 123.2, 123.0, 109.5, 108.5, 108.3, 106.9, 105.7, 101.4, 81.9 (d, J = 171 Hz), 68.6 (d, J = 21 Hz), 60.8, 56.0, 55.4, 32.0. ^{19}F NMR ($CDCl_3$) δ = −224.0. MS (EI): m/z = 561 $[M+Na]^+$, 521 $[M-H_2O]^+$. Anal. Calcd for $C_{29}H_{27}FO_9$: C, 64.68; H, 5.05. Found: C, 64.48; H, 4.93.

4.2.7. 3-Benzo[1,3]dioxol-5-yl-4-[3-(2-bromoethoxy)-4,5-dimethoxybenzyl]-5-hydroxy-5-(4-methoxyphenyl)-5H-furan-2-one 8

A suspension of 1.50 g (5.18 mmol) of 3-(2-bromoethoxy)-4,5-dimethoxybenzaldehyde **6**, 286 mg (5.30 mmol) sodium methylate and 1.78 g (5.20 mmol) of 2-(1,3-benzodioxol-5-yl)-1-(4-methoxyphenyl)-4-oxobutyric acid methyl ester **1a** in 40 ml of methanol is refluxed for 40 h under argon. Acetic acid (≈3.0 ml) is added and the mixture is refluxed for further 8 h. The reaction mixture is poured onto ice and extracted with ethyl acetate. The combined organic phases are washed with saturated bicarbonate solution and brine and dried over magnesium sulfate. After filtration and removal of the solvent the crude residue is chromatographed on silica gel (cyclohexane/ethyl acetate 3/1, R_f = 0.29) to yield 1.60 g (2.67 mmol, 52%) of the product as a white powder, mp 64 °C. ^1H NMR ($CDCl_3$) δ = 7.35 (d, 2H, J = 9.0 Hz), 6.92–6.86 (m, 2H), 6.82 (d, 2H, J = 9.0 Hz), 6.77 (d, 1H, J = 7.6 Hz), 5.98 (s, 2H), 6.01 (m, 1H), 5.97 (m, 1H), 5.94 (s, 2H), 4.30 (s, br, 1H), 4.04 (m, 2H), 3.77 (s, 3H), 3.74 (s, 3H), 3.63 (d, 2H, J = 11.4 Hz), 3.60 (s, 3H), 3.54 (t, 2H, J = 6.0 Hz). ^{13}C NMR ($CDCl_3$) δ = 170.9, 160.4, 160.1, 153.1, 151.3, 148.1, 147.7, 137.3, 131.8, 128.6, 128.2, 127.3, 123.1, 122.8, 113.9, 109.3, 108.4, 108.1, 106.8, 105.5, 101.3, 69.0, 60.9, 55.9, 55.3, 31.8, 29.1. MS (EI): m/z = 623 $[M+Na]^+$ (^{79}Br), 621 $[M+Na]^+$ (^{81}Br), 583 $[M-OH]^+$ (^{81}Br), 581 $[M-OH]^+$ (^{79}Br). Anal. Calcd for $C_{29}H_{27}BrO_9$: C, 58.11; H, 4.54. Found: C, 58.25; H, 4.64.

4.2.8. 3-Benzo[1,3]dioxol-5-yl-5-[4-(2-fluoroethoxy)phenyl]-5-hydroxy-4-(3,4,5-trimethoxybenzyl)-5H-furan-2-one 9

To a suspension of 585 mg (1.61 mmol) of 2-(1,3-benzodioxol-5-yl)-1-[4-(2-fluoroethoxy)phenyl]-4-oxobutyric acid methyl ester **2** and 91 mg (1.68 mmol) sodium methylate in 20 ml methanol 320 mg (1.63 mmol) of 3,4,5-trimethoxybenzaldehyde (**4**, *FLUKA*) are added. The mixture is refluxed for 12 h under argon. Acetic acid (≈0.8 ml) is added and the mixture is further refluxed for 5 h. The reaction mixture is poured onto ice and extracted with ethyl acetate. The combined organic phases are washed with saturated bicarbonate solution and brine and dried over magnesium sulfate. After filtration and removal of the solvent the residue is chromatographed on silica gel (petroleum ether/ethyl acetate 1/1, R_f = 0.26) to yield 250 mg (0.46 mmol, 29%) of the product as a light yellow powder, mp 196 °C (decomp.). ^1H NMR ($CDCl_3$) δ = 7.39 (d, 2H, J = 8.9 Hz), 6.94 (dd, 1H, J = 8.1 Hz, J = 1.7 Hz), 6.91 (d, 1H, J = 1.7 Hz), 6.85 (d, 2H, J = 8.9 Hz), 6.79 (d, 1H, J = 8.1 Hz), 6.00 (s, 2H), 5.95 (s, 2H), 4.88 (s, br, 1H), 4.73 (dm, 2H, J = 47 Hz), 4.17 (dm, 2H, J = 28 Hz), 3.73 (s, 3H), 3.68 (s, 2H), 3.63 (s, 3H). ^{13}C NMR ($CDCl_3$) δ = 171.2, 160.3, 159.2, 152.9, 148.2, 147.7, 136.7, 131.8, 129.6, 128.2, 127.5, 123.1, 123.0, 114.5, 109.4, 108.4, 106.0, 105.6, 101.3, 81.7 (d, J = 171 Hz), 67.3 (d, J = 20 Hz), 60.7, 55.9, 32.1. ^{19}F NMR ($CDCl_3$) δ = −224.0. MS (EI): m/z = 561 $[M+Na]^+$, 521 $[M-H_2O]^+$. Anal. Calcd for $C_{29}H_{27}FO_9$: C, 64.68; H, 5.05. Found: C, 64.44; H, 4.88.

4.2.9. 3-Benzo[1,3]dioxol-5-yl-5-hydroxy-5-[4-(2-bromoethoxy)-phenyl]-4-(3,4,5-trimethoxybenzyl)-5H-furan-2-one 10

To a suspension of 3.00 g (6.89 mmol) of 2-(1,3-benzodioxol-5-yl)-1-[4-(2-bromoethoxy)phenyl]-4-oxobutyric acid methyl ester **3** and 432 mg (8.00 mmol) sodium methylate in 50 ml methanol 1.37 g (7.00 mmol) of 3,4,5-trimethoxybenzaldehyde (**4**, *FLUKA*) are added. The mixture is refluxed for 24 h under argon. Acetic acid (≈3.0 ml) is added and the mixture is refluxed for further 6 h. The reaction mixture is poured onto ice and extracted with ethyl acetate. The combined organic phases are washed with saturated bicarbonate solution and brine and dried over magnesium sulfate. After filtration and removal of the solvent the crude residue is chromatographed on silica gel (cyclohexane/ethyl acetate 2/1, R_f = 0.26) to yield 1.70 g (2.80 mmol, 41%) of the product as a white powder, mp 178 °C. ^1H NMR ($CDCl_3$ + 10% DMSO-d_6) δ = 7.37 (d, 2H, J = 9.0 Hz), 6.94–6.88 (m, 2H), 6.85 (d, 2H, J = 9.0 Hz), 6.81 (d, 1H, J = 7.9 Hz), 5.98 (s, 2H), 5.92 (s, 2H), 4.29 (t, 2H, J = 6.3 Hz), 3.76 (d, 1H, J = 15.9 Hz), 3.68 (t, 2H, J = 6.3 Hz), 3.64 (s, 3H), 3.59 (s, 6H), 3.51 (d, 1H, J = 15.9 Hz). The signal of the proton of the hydroxy group is not detected. ^{13}C NMR ($CDCl_3$ + 10% DMSO-d_6) δ = 170.0, 160.3, 157.2, 151.1, 146.5, 146.2, 134.6, 130.7, 128.8, 126.5, 126.1, 122.2, 121.8, 113.0, 108.1, 106.9, 104.7, 104.6, 100.0, 66.6, 59.2, 54.4, 30.8, 28.6. MS (EI): m/z = 623 $[M+Na]^+$ (^{79}Br), 621 $[M+Na]^+$ (^{81}Br). Anal. Calcd for $C_{29}H_{27}BrO_9$: C, 58.11; H, 4.54. Found: C, 58.28; H, 4.61.

4.2.10. 2-(5-{[4-(Benzo[1,3]dioxol-5-yl)-2-hydroxy-2-(4-methoxyphenyl)-5-oxo-2,5-dihydrofuran-3-yl]methyl}-2,3-dimethoxyphenoxy)ethyl 4-methylbenzenesulfonate 11

A mixture of 1.45 g (2.42 mmol) of the bromide 3-benzo[1,3]-dioxol-5-yl-4-[3-(2-bromoethoxy)-4,5-dimethoxybenzyl]-5-hydroxy-5-(4-methoxyphenyl)-5*H*-furan-2-one **8** and 6.75 g (24.0 mmol) silver-4-methylbenzene sulfonate in 100 ml of acetonitrile is heated to reflux for 17 h. After filtration to remove the silver bromide and evaporation of the solvent acetone is added. The precipitate (excess silver-4-methylbenzenesulfonate) is removed by filtration and the solvent is evaporated. Purification of the crude product by silica gel column chromatography (cyclohexane/ethyl acetate 3/2, R_f = 0.21) yields the product as a white foam (1.30 g, 1.88 mmol, 78%), mp 64 °C (decomp.). ^1H NMR ($CDCl_3$) δ = 7.76 (d, 2H, J = 8.2 Hz), 7.34 (d, 2H, J = 8.7 Hz), 7.30 (d, 2H, J = 8.2 Hz), 6.88–6.83 (m, 2H), 6.80 (d, 2H, J = 8.7 Hz), 6.74 (d, 1H, J = 7.9 Hz), 5.98 (m, 1H), 5.95 (m, 1H), 5.92 (s, 2H), 4.68 (s, br, 1H), 4.23 (t, 2H, J = 4.7 Hz), 3.94 (m, 2H), 3.75 (s, 3H), 3.63 (s, 3H), 3.60–3.56 (m, 2H), 3.58 (s, 3H), 2.40 (s, 3H). ^{13}C NMR ($CDCl_3$) δ = 171.2, 160.4, 153.1, 151.4, 148.2, 147.7, 145.1, 137.3, 132.8, 131.9, 130.0, 128.7,

128.3, 127.9, 127.5, 123.2, 122.9, 114.0, 109.5, 108.4, 108.3, 107.0, 105.8, 101.4, 68.3, 66.8, 60.8, 56.0, 55.4, 32.0, 21.6. The signal of one quaternary carbon atom is not detected. MS (EI): m/z = 713 $[M+Na]^+$, 673 $[M-OH]^+$. Anal. Calcd for $C_{36}H_{34}O_{12}S$: C, 62.60; H, 4.96. Found: C, 62.28; H, 4.84.

4.2.11. 2-{4-[4-(Benzo[1,3]dioxol-5-yl)-2-hydroxy-5-oxo-3-(3,4,5-trimethoxybenzyl)-2,5-dihydro-furan-2-yl]phenoxy}ethyl 4-methylbenzenesulfonate 12

A mixture of 800 mg (1.33 mmol) of the bromide 3-benzo[1,3]-dioxol-5-yl-5-hydroxy-5-[4-(2-bromoethoxy)phenyl]-4-(3,4,5-trimethoxybenzyl)-5*H*-furan-2-one **10** and 3.9 g (13.0 mmol) silver-4-methylbenzene sulfonate in 80 ml of acetonitrile is heated to reflux for 17 h. After filtration to remove the silver bromide and evaporation of the solvent acetone is added. The precipitate (excess silver-4-methylbenzenesulfonate) is removed by filtration and the solvent is evaporated. Purification of the crude product by silica gel column chromatography (cyclohexane/ethyl acetate 3/2, R_f = 0.18) yields the product as a white foam (750 mg, 1.09 mmol, 82%), mp 68 °C (decomp.). ^{1}H NMR ($CDCl_3$) δ = 7.78 (d, 2H, J = 8.0 Hz), 7.32 (dd, 1H, J = 8.8 Hz, J = 2.5 Hz), 6.92–6.86 (m, 2H), 6.75 (d, 2H, J = 8.0 Hz), 6.79 (d, 2H, J = 8.8 Hz), 5.94 (s, 2H), 5.92 (s, 2H), 4.31 (dd, 2H, J = 3.6 Hz, J = 5.4 Hz), 4.08 (dd, 2H, J = 3.6 Hz, J = 5.4 Hz), 3.67 (s, 3H), 3.62 (s, 2H), 3.57 (s, 6H), 2.42 (s, 3H). The proton signal of the hydroxy group is not detected. ^{13}C NMR ($CDCl_3$) δ = 171.2, 160.6, 158.7, 152.7, 148.0, 147.6, 145.1, 136.3, 132.6, 131.8, 129.9, 129.6, 128.0, 127.9, 127.5, 123.1, 122.9, 114.4, 109.4, 108.4, 105.7, 101.3, 67.9, 65.5, 60.7, 55.8, 32.0, 21.6. The signal of one quaternary carbon atom is not detected. MS (EI): m/z = 713 $[M+Na]^+$. Anal. Calcd for $C_{36}H_{34}O_{12}S$: C, 62.60; H, 4.96. Found: C, 62.24; H, 5.01.

4.3. Radiochemistry

The production of no-carrier-added aqueous [^{18}F]fluoride ion was achieved on a CTI RDS111e cyclotron by irradiation of a 1.2 ml water target using 10 MeV proton beams on 97.0% enriched [^{18}O]water by the ^{18}O(p,n)^{18}F nuclear reaction. A typical batch was 9.4 GBq of [^{18}F]fluoride ion at the end of radionuclide production for currents of 27 μA and irradiation times of 20 min. The radiosynthesis of 3-benzo[1,3]dioxol-5-yl-4-[3-(2-[^{18}F]fluoroethoxy)-4,5-dimethoxybenzyl]-5-hydroxy-5-(4-methoxyphenyl)-5H-furan-2-one [^{18}F]7, and 3-benzo[1,3]dioxol-5-yl-5-[4-(2-[^{18}F]fluoroethoxy)phenyl]-5-hydroxy-4-(3,4,5-trimethoxy-benzyl)-5H-furan-2-one [^{18}F]9 was accomplished using a computer controlled TRACERlab FX_{FDG} Synthesizer (GE Healthcare Germany, München, Germany). The batch of aqueous [^{18}F]fluoride ion was passed through an anion exchange resin (Sep-Pak® Light Waters Accell™ Plus QMA cartridge, preconditioned with 5 ml 1.0 M K_2CO_3 and 10 ml water). [^{18}F]Fluoride ion was eluted from the resin with a mixture of 40 μl 1 M K_2CO_3, 200 μl water for injection, and 800 μl DNA-grade acetonitrile containing 18 mg Kryptofix® 2.2.2. Subsequently, the aqueous [^{18}F]K(Kryptofix 2.2.2)F solution was carefully evaporated to dryness in vacuo. Compound [^{18}F]7 was prepared by treating 1.7 mg (2.98 μmol) tosylate precursor **11** with the dried [^{18}F]K(Kryptofix 2.2.2)F residue in 1 ml DNA-grade acetonitrile at 84 °C for 5 min. After cooling to RT the crude reaction mixture was diluted with 10 ml water for injection and passed through a Waters Sep-Pak® Light C18 cartridge (preconditioned with 10 ml of ethanol and 10 ml of water for injection). The cartridge was washed with additional 10 ml water for injection, followed by elution of raw [^{18}F]7 with 0.8 ml of acetonitrile (DNA-grade). An amount of 200 μl of the solution was fractionized using a gradient radio-HPLC procedure (conditions: λ = 254 nm; flow = 1.5 ml/min; column: Nucleosil 100-5 C18 (250 × 4.6 mm^2); eluents: A, water for injection/trifluoroacetic acid (TFA) 1000/1 (v/v); B, acetonitrile/TFA 1000/1 (v/v); elution gradient: 70% A for 4 min, A from 70% to 5% in 38 min, 5% A for 2 min, from 5% to 70% A in 1 min) resulting in **[^{18}F]7** with a radiochemical yield of 21.4 ± 6.1% (mean ± SD, decay-corrected, n = 12) and a radiochemical purity >98% (retention time t_R = 27.0 min). The time of synthesis and purification was ≈70 min from the end of radionuclide production. The determined specific radioactivity was 35–50 GBq/μmol at the end of synthesis. The specific activity of **[^{18}F]7** was estimated by comparing the peak area of the UV-trace of purified **[^{18}F]7** with a standard curve of known concentrations of reference compound **7** realized with the above mentioned RP-HPLC system and the described conditions. The chemical identity of **[^{18}F]7** was proved by co-injection and co-elution of **[^{18}F]7** and non-radioactive counterpart **7** on the mentioned HPLC system. For animal studies, the product fraction of the HPLC purification procedure was collected, evaporated to dryness and reconstituted in 10% ethanol/water for injection (v/v). Derivative **[^{18}F]9** was prepared and purified by the same reaction conditions as stated above for **[^{18}F]7**. The radiochemical yield was ≈12% (decay-corrected, n = 3) and the radiochemical purity was >98% (retention time t_R = 29.2 min). The time of synthesis and purification was ≈70 min from the end of radionuclide production. The specific radioactivity was not determined. The chemical identity of **[^{18}F]9** was proved by co-injection and co-elution of **[^{18}F]9** and non-radioactive counterpart **9** on the mentioned HPLC system.

4.4. Biology

In vitro determination of receptor affinities: Microsomes were prepared by homogenizing ventricles from DBA mice at 4 °C for 90 s in 1 ml of buffer A (10 mM EDTA, 10 mM HEPES, 0.1 mM benzamidine, pH 7.4), using a Polytron PT 3000 (Kinematica, Lucerne, Switzerland). Homogenates were centrifuged at 45,000*g* for 15 min at 4 °C. The pellets were resuspended in 1 ml of buffer B (1 mM EDTA, 10 mM HEPES, 0.1 mM benzamidine, pH 7.4) and recentrifuged at 45,000*g* for 15 min at 4 °C. The pellets were resuspended in 1 ml of buffer B and centrifuged at 10,000*g* for 10 min at 4 °C. The supernatants were recentrifuged at 45,000*g* for 15 min at 4 °C. The pellets, partially enriched membranes, were resuspended in buffer C (50 mM Tris–HCl, 5 mM $MgCl_2$, pH 7.4), and stored frozen at −80 °C. For competition binding studies, the prepared membranes were resuspended in buffer D (10 mM Tris–HCl, 154 mM NaCl, 0.1 mM ascorbic acid, pH 7.4) at 0 °C. An amount of 10 μg of membranes were incubated with 40 pM of [^{125}I]ET-1 (Perkin–Elmer Live Sciences Inc., Billerica, MA, USA) and with varying concentrations (10 pM–100 μM) of ligands **7**–**12** at 37 °C for 4 h. Reactions were stopped by filtering onto Whatman GF/B filters and washed with 0.9% NaCl at 4 °C. The membrane bound radioactivity was determined in a γ-scintillation counter. Competition binding curves were analyzed by nonlinear regression analysis using the XMGRACE program (Linux software). The high- and low-affinity IC_{50} values were converted into the high- and low-affinity inhibition constants ($K_i(ET_A)$and $K_i(ET_B)$) by the method of Cheng–Prusoff[39] using the previously determined K_D value of [^{125}I]ET-1 (208 ± 2 pM).[34]

Biodistribution studies: Adult C57BL/6 mice (male and female, 25–30 g) were anesthetized by isoflurane/N_2O/O_2 and one lateral tail was canulated (27 G *VenofixA* needle with 20 cm polythene catheter tubing, od 1 mm, id 0.38 mm). Animals were allowed to recover from the anesthesia for ∼1 h and during the studies they were conscious but under light restraint. The radiofluorinated ET_A ligand **[^{18}F]7** (0.2–2.0 MBq at injection, 0.3–1.0 nmol/kg) was injected as a bolus (2.0 μl/g, 100 μl saline flush) via the tail vein. Some animals received PD 156707 at 1.0 μmol/kg (n = 7) or vehicle (water for injection, n = 7) as an iv bolus (1.0 μl/g, 100 μl saline flush) 10 min before **[^{18}F]7**. Aliquots of each injectate were diluted in saline and

measured to determine the radioactivity injected into each animal. At selected times after injection of the radioligand, animals were killed by intravenous injection of sodium pentobarbitone (Euthatal) at 200 mg/kg and tissues were rapidly removed. Tissue samples were blotted and transferred to weighed vials for reweighing and measurement of radioactivity using an automated gamma counter (Wallac Wizard 3″, Perkin–Elmer Life Sciences, Boston, USA). Radioactivity was expressed as an uptake index, defined as

$$\text{Uptake index} = \frac{\text{Tissue radioactivity (cpm)/Tissue wet weight (g)}}{\text{Radioactivity injected (cpm)/Body weight (g)}}$$

Metabolism: Rat plasma. One male Wistar rat (Charles River Laboratories, Sulzfeld, Germany, 350 g) was anesthetized by isoflurane/N_2O/O_2 and blood (10 ml) was removed by cardiac puncture. Plasma was separated by centrifugation (10,000*g* for 4 min) and stored at −20 °C overnight. Samples (0.5 ml) were incubated with 19 MBq of the radioligand **[^{18}F]7** at 37 °C using an *Eppendorf* Thermomixer comfort (*Eppendorf AG*, Hamburg, Germany). At different time points (1, 2.5, 20, and 60 min) proteins were precipitated by addition of ice-cold acetonitrile (700 μl) and centrifugation at 10,000*g* for 4 min. The supernatant was separated and the radioactivity of the protein pellet and the supernatant was measured (Ionization chamber 637620, MED Nuklearmedizin-Technik GmbH, Dresden, Germany) to estimate protein binding. A sample of each supernatant (200 μl) was analyzed by HPLC (conditions see above).

Mouse: Adult C57BL/6 mice (male and female, 25–30 g) were prepared in accordance with the chapter biodistribution (see above). **[^{18}F]7** was injected as a bolus (100 μl) via the tail vein. Aliquots of each injectate were diluted in saline and measured to determine the radioactivity injected into each animal. Animals were sacrificed at 5 or 20 min after injection of the radiotracer by intravenous injection of sodium pentobarbitone (Euthatal) at 200 mg/kg. Blood was taken immediately by cardiac puncture and centrifuged at 10,000*g* for 4 min (*Eppendorf* centrifuge 5415D, *Eppendorf AG*, Hamburg, Germany) to separate plasma. Plasma from two mice was pooled for analysis by HPLC. Ice-cold acetonitrile (0.7 ml) was added to the pooled plasma (0.7–1.0 ml) and the precipitated proteins were removed by centrifugation (10,000*g* for 4 min). A sample of the resulting supernatant (200 μl) was spiked with non-radioactive **7** (10 μg) and analyzed by HPLC (conditions see above). In addition, urine samples were taken at the given time points from one mouse each and analyzed by HPLC (conditions see above).

Rat. One male Wistar rat (Charles River Laboratories, Sulzfeld, Germany, 400 g) was used for the experiment. The animal was anesthetized by isoflurane/N_2O/O_2 for insertion of catheters (see above) into the ventral tail artery and one lateral tail vein and were allowed to recover from the anesthesia for ≈2 h. An amount of 40 MBq of **[^{18}F]7** was injected as a bolus via the tail vein. Four blood samples (600–800 μl) were collected from the tail artery catheter at 2.5, 10, 20, and 60 min after injection. Cell free plasma was obtained by centrifugation at 10,000*g* for 4 min. Ice-cold acetonitrile (0.7 ml) was added to the plasma and the precipitated proteins were removed by centrifugation (10,000*g* for 4 min). A sample of the resulting supernatant (200 μl) was spiked with non-radioactive **7** (10 μg) and analyzed by HPLC (conditions see above). At 60 min the animal was killed by intravenous injection of sodium pentobarbitone (Euthatal) at 200 mg/kg. A urine sample was taken by puncture of the bladder and was directly injected into the HPLC for analysis.

4.5. PET scans

Uptake of radioactivity after intravenous injection of ET_A ligand **[^{18}F]7** was visualized using the high-resolution quadHIDAC small-animal PET scanner.[40] C57BL/6 mice (female, 22−23 g) were anesthetized by inhalation (isoflurane 2%, oxygen 0.5 l min^{-1}) for insertion of catheters into tail veins and subsequent PET scanning. Two mice were positioned in parallel in the scanner and 30 s after start of the acquisition the radioligand **[^{18}F]7** (6.6 MBq in 100 μl, 100 μl saline flush) was injected into each mouse simultaneously. List mode data were acquired for 2 h and reconstructed into 10 min time frames using an iterative reconstruction algorithm.[41] PET images were analyzed using in-house software programs in MATLAB (The MathWorks Company, Natick, MA) and C programming languages.[42] For in vivo biodistribution measurements ROIs were drawn over the respective organs in five different coronal planes and analyzed as above.

Acknowledgements

This study was in part supported by the Deutsche Forschungsgemeinschaft (DFG), project SCHA 758-5-1, DFG Sonderforschungsbereich SFB 656, Münster, Germany (subprojects A1 and A4), the Interdisziplinäres Zentrum für Klinische Forschung (IZKF), Münster, Germany (core unit SmAP) and the Bundesministerium für Bildung und Forschung (BMBF), Germany (MoBiMed subproject 01EZ0807). The authors wish to thank Sandra Schröer, Anne Kanzog, and Christine Bätza for technical support.

References and notes

1. Hickey, K. A.; Rubanyi, G.; Paul, R. J.; Highsmith, R. F. *Am. J. Physiol.* **1985**, *248*, C550.
2. Yanagisawa, M.; Kurihara, H.; Kimura, S.; Tomobe, Y.; Kobayashi, M.; Mitsui, Y.; Yazaki, Y.; Goto, K.; Masaki, T. *Nature* **1988**, *332*, 411.
3. Bousette, N.; Giaid, A. *Can. J. Physiol. Pharmacol.* **2003**, *81*, 578.
4. Giaid, A. *Chest* **1998**, *114*, 208S.
5. Giaid, A.; Yanagisawa, M.; Langleben, D.; Michel, R. P.; Levy, R.; Shennib, H.; Kimura, S.; Masaki, T.; Duguid, W. P.; Stewart, D. J. *N. Eng. J. Med.* **1993**, *328*, 1732.
6. Saito, Y.; Nakao, K.; Mukoyama, M.; Imura, H. *N. Eng. J. Med.* **1990**, *322*, 205.
7. Teerlink, J. R.; Loffler, B. M.; Hess, P.; Maire, J. P.; Clozel, M.; Clozel, J. P. *Circulation* **1994**, *90*, 2510.
8. Yoshibayashi, M.; Nishioka, K.; Nakao, K.; Saito, Y.; Matsumura, M.; Ueda, T.; Temma, S.; Shirakami, G.; Imura, H.; Mikawa, H. *Circulation* **1991**, *84*, 2280.
9. Bagnato, A.; Natali, P. G. *Cancer Treat. Res.* **2004**, *119*, 293.
10. Bagnato, A.; Natali, P. G. *J. Transl. Med.* **2004**, *2*, 16.
11. Nelson, J.; Bagnato, A.; Battistini, B.; Nisen, P. *Nat. Rev. Cancer* **2003**, *3*, 110.
12. Rosano, L.; Spinella, F.; Di Castro, V.; Nicotra, M. R.; Albini, A.; Natali, P. G.; Bagnato, A. *Am. J. Pathol.* **2003**, *163*, 753.
13. Smollich, M.; Wülfing, P. *Curr. Vasc. Pharmacol.* **2007**, *5*, 239.
14. Dupuis, J.; Goresky, C. A.; Fournier, A. *J. Appl. Physiol.* **1996**, *81*, 1510.
15. Dupuis, J.; Stewart, D. J.; Cernacek, P.; Gosselin, G. *Circulation* **1996**, *94*, 1578.
16. Fukuroda, T.; Fujikawa, T.; Ozaki, S.; Ishikawa, K.; Yano, M.; Nishikibe, M. *Biochem. Biophys. Res. Commun.* **1994**, *199*, 1461.
17. Langleben, D.; Dupuis, J.; Hirsch, A.; Giovinazzo, M.; Langleben, I.; Khoury, J.; Ruel, N.; Caron, A. *Chest* **2005**, *128*, 622S.
18. Polikepahad, S.; Moore, R. M.; Venugopal, C. S. *Res. Commun. Mol. Pathol. Pharmacol.* **2006**, *119*, 3.
19. Barton, M.; Haudenschild, C. C.; d'Uscio, L. V.; Shaw, S.; Munter, K.; Lüscher, T. F. *Proc. Natl. Acad. Sci. U.S.A.* **1998**, *95*, 14367.
20. d'Uscio, L. V.; Barton, M.; Shaw, S.; Lüscher, T. F. *Cardiovasc. Res.* **2002**, *53*, 487.
21. Iwasa, S.; Fan, J.; Miyauchi, T.; Watanabe, T. *Pathobiology* **2001**, *69*, 1.
22. Maguire, J. J.; Wiley, K. E.; Kuc, R. E.; Stoneman, V. E.; Bennett, M. R.; Davenport, A. P. *Exp. Biol. Med. (Maywood)* **2006**, *231*, 806.
23. Alanen, K.; Deng, D. X.; Chakrabarti, S. *Histopathology* **2000**, *36*, 161.
24. Asham, E.; Shankar, A.; Loizidou, M.; Fredericks, S.; Miller, K.; Boulos, P. B.; Burnstock, G.; Taylor, I. *Br. J. Cancer* **2001**, *85*, 1759.
25. Bagnato, A.; Salani, D.; Di Castro, V.; Wu-Wong, J. R.; Tecce, R.; Nicotra, M. R.; Venuti, A.; Natali, P. G. *Cancer Res.* **1999**, *59*, 720.
26. Nelson, J. B.; Chan-Tack, K.; Hedican, S. P.; Magnuson, S. R.; Opgenorth, T. J.; Bova, G. S.; Simons, J. W. *Cancer Res.* **1996**, *56*, 663.
27. Wülfing, P.; Diallo, R.; Kersting, C.; Wülfing, C.; Poremba, C.; Rody, A.; Greb, R. R.; Bocker, W.; Kiesel, L. *Clin. Cancer Res.* **2003**, *9*, 4125.
28. Aleksic, S.; Szabo, Z.; Scheffel, U.; Ravert, H. T.; Mathews, W. B.; Kerenyi, L.; Rauseo, P. A.; Gibson, R. E.; Burns, H. D.; Dannals, R. F. *J. Nucl. Med.* **2001**, *42*, 1274.
29. Johnstrøm, P.; Fryer, T. D.; Richards, H. K.; Barret, O.; Clark, J. C.; Ohlstein, E. H.; Pickard, J. D.; Davenport, A. P. *J. Cardiovasc. Pharmacol.* **2004**, *44*, S34.
30. Mathews, W. B.; Zober, T. G.; Ravert, H. T.; Scheffel, U.; Hilton, J.; Sleep, D.; Dannals, R. F.; Szabo, Z. *Nucl. Med. Biol.* **2006**, *33*, 15.

31. Mathews, W. B.; Murugesan, N.; Xia, J.; Scheffel, U.; Hilton, J.; Ravert, H. T.; Dannals, R. F.; Szabo, Z. *J. Nucl. Med.* **2008**, *49*, 1529.
32. Doherty, A. M.; Patt, W. C.; Edmunds, J. J.; Berryman, K. A.; Reisdorph, B. R.; Plummer, M. S.; Shahripour, A.; Lee, C.; Cheng, X. M.; Walker, D. M., et al *J. Med. Chem.* **1995**, *38*, 1259.
33. Patt, W. C.; Edmunds, J. J.; Repine, J. T.; Berryman, K. A.; Reisdorph, B. R.; Lee, C.; Plummer, M. S.; Shahripour, A.; Haleen, S. J.; Keiser, J. A.; Flynn, M. A.; Welch, K. M.; Reynolds, E. E.; Rubin, R.; Tobias, B.; Hallak, H.; Doherty, A. M. *J. Med. Chem.* **1997**, *40*, 1063.
34. Höltke, C.; Law, M. P.; Wagner, S.; Breyholz, H. J.; Kopka, K.; Bremer, C.; Levkau, B.; Schober, O.; Schäfers, M. *Bioorg. Med. Chem.* **2006**, *14*, 1910.
35. Höltke, C.; Waldeck, J.; Kopka, K.; Heindel, W.; Schober, O.; Schäfers, M.; Bremer, C. *Mol. Imaging* **2009**, *8*, 27.
36. Zoghbi, S. S.; Shetty, H. U.; Ichise, M.; Fujita, M.; Imaizumi, M.; Liow, J. S.; Shah, J.; Musachio, J. L.; Pike, V. W.; Innis, R. B. *J. Nucl. Med.* **2006**, *47*, 520.
37. Sykes, T. R.; Ruth, T. J.; Adam, M. J. *Int. J. Rad. Appl. Instrum. B* **1986**, *13*, 497.
38. Parenty, A. D.; Smith, L. V.; Pickering, A. L.; Long, D. L.; Cronin, L. *J. Org. Chem.* **2004**, *69*, 5934.
39. Cheng, Y.; Prusoff, W. H. *Biochem. Pharmacol.* **1973**, *22*, 3099.
40. Schäfers, K. P.; Reader, A. J.; Kriens, M.; Knoess, C.; Schober, O.; Schäfers, M. *J. Nucl. Med.* **2005**, *46*, 996.
41. Reader, A. J.; Ally, S.; Bakatselos, F.; Manavaki, R.; Walledge, R. J.; Jeavons, A. P.; Julyan, P. J.; Zhao, S.; Hastings, D. L.; Zweit, J. *IEEE Trans. Nucl. Sci.* **2002**, *49*, 693.
42. Biedenstein, S.; Schäfers, M.; Stegger, L.; Kuwert, T.; Schober, O. *Eur. J. Nucl. Med.* **1999**, *26*, 201.